

Measuring the Cosmic Ray Muon-Induced Fast Neutron Spectrum by (n,p) Isotope Production Reactions in Underground Detectors

Cristiano Galbiati*

Department of Physics, Princeton University, Princeton, NJ 08544, USA

John F. Beacom†

*Department of Physics, Ohio State University, Columbus, OH 43210, USA and
Department of Astronomy, Ohio State University, Columbus, OH 43210, USA*

(Dated: October 24, 2018)

While cosmic ray muons themselves are relatively easy to veto in underground detectors, their interactions with nuclei create more insidious backgrounds via: (i) the decays of long-lived isotopes produced by muon-induced spallation reactions inside the detector, (ii) spallation reactions initiated by fast muon-induced neutrons entering from outside the detector, and (iii) nuclear recoils initiated by fast muon-induced neutrons entering from outside the detector. These backgrounds, which are difficult to veto or shield against, are very important for solar, reactor, dark matter, and other underground experiments, especially as increased sensitivity is pursued. We used FLUKA to calculate the production rates and spectra of all prominent secondaries produced by cosmic ray muons, in particular focusing on secondary neutrons, due to their importance. Since the neutron spectrum is steeply falling, the total neutron production rate is sensitive just to the relatively soft neutrons, and not to the fast-neutron component. We show that the neutron spectrum in the range ~ 10 – 100 MeV can instead be probed by the (n,p) -induced isotope production rates $^{12}\text{C}(n,p)^{12}\text{B}$ and $^{16}\text{O}(n,p)^{16}\text{N}$ in oil- and water-based detectors. The result for ^{12}B is in good agreement with the recent KamLAND measurement. Besides testing the calculation of muon secondaries, these results are also of practical importance, since ^{12}B ($T_{1/2} = 20.2$ ms, $Q = 13.4$ MeV) and ^{16}N ($T_{1/2} = 7.13$ s, $Q = 10.4$ MeV) are among the dominant spallation backgrounds in these detectors.

PACS numbers: 25.30.Mr, 25.40.Sc, 25.20.-x, 96.40.Tv

Keywords: Muon-induced nuclear reactions; Spallation reactions; Low-background experiments

I. INTRODUCTION

To reduce the cosmic-ray muon background, experiments to measure rare processes must be sited underground, where the muon flux is greatly attenuated, and surrounded by an active veto system, to tag the residual muons. Even with these standard measures, muons are still responsible for significant backgrounds in underground experiments, via the secondary particles created by muon interactions with nuclei. If the muon interacts inside the detector, the secondary shower particles create unstable isotopes; some have long lifetimes, making it hard to associate them with particular muons. If the muon interacts outside the detector, it cannot be tagged, and “invisible” secondaries, especially neutrons, can penetrate the detector shielding. These neutrons can then initiate spallation reactions or nuclear recoils inside the detector. While these muon-induced backgrounds are already given serious consideration at present, the next generation of underground neutrino, dark matter, and double-beta decay experiments will require both lower backgrounds and a better quantitative understanding of their characteristics.

Fundamental to understanding these backgrounds is the rate and spectrum of muon-induced neutrons [1]. The neutron spectrum is steeply falling over orders of magnitude in neutron energy, but not uniformly so, indicating complexity in its formation. The total rate of neutron production depends primarily on the soft-neutron spectrum, and has been well measured. In Table I we summarize the main characteristics of the muon flux underground at several relevant depths [2–9]. With increasing depth, the muon flux falls quickly and the muon average energy rises at first quickly and then much more slowly. The capture rates of neutrons produced by muons are also noted. The Gran Sasso rate was measured with the Borexino Counting Test Facility [10–12]. The rates at other depths were calculated using the scaling law given by Ref. [1]; the result for Kamioka is fully consistent with the rate of 2940/kton day measured by KamLAND [13].

What is needed now is a more quantitative understanding of the neutron spectrum at moderate and high energies, as emphasized by Ref. [14]. In this paper, we consider the production of unstable isotopes as a new and direct probe of the moderate-energy neutron spectrum. We focus our attention here on the (n,p) reactions in oil- and water-based detectors, and show that their rates are a sensitive probe of the ~ 10 – 100 MeV neutron spectrum, which we calculate using FLUKA. The predicted rate of $^{12}\text{C}(n,p)^{12}\text{B}$ production is in very good agreement with the rate measured in the KamLAND experiment [13].

*Email address: galbiati@princeton.edu

†Email address: beacom@mps.ohio-state.edu

TABLE I: Depth, muon flux, muon average energy, and neutron capture rate at sea level, 500 m.w.e., and the Kamioka, Gran Sasso, and Sudbury underground laboratories.

	Depth [m.w.e.]	Φ_μ [$\mu/\text{m}^2 \text{ h}$]	$\langle E_\mu \rangle$ [GeV]	$p(n, \gamma)d$ [events/kton day]
Sea Level	0	6.0×10^5	4	7.2×10^6
500 m.w.e.	500	610	100	8.0×10^4
Kamioka	2700	9.6	285	3000
Gran Sasso	3800	1.2	320	400
SNOlab	6000	0.012	350	4.3

These *in-situ* measurements are an important complement to measurements made at accelerators, namely the experiment of Ref. [2] at CERN using muon beam energies of 100 and 190 GeV.

The ultimate goal of these studies is to characterize the muon-induced neutron spectrum precisely, at all energies, as well as the yields of unstable isotopes produced by muon secondaries. Here we make a step towards this goal by focusing on the reactions $^{12}\text{C}(n, p)^{12}\text{B}$ and $^{16}\text{O}(n, p)^{16}\text{N}$ in oil- and water-based detectors. We show below that at depths greater than a few hundred m.w.e., these are the only significant production channels for ^{12}B in oil-based detectors and ^{16}N in water-based detectors, respectively. These are among the most significant spallation products in these two important types of detectors. By considering these single isotopes, with the same masses as the parents, we can isolate just the (n, p) production channel, and hence directly probe the muon-induced neutron spectrum. Even though the rates of these (n, p) reactions are well below the total neutron production rates, they are still quite large: about 60/kton/day (calculated and measured) for ^{12}B in KamLAND [13], and 50/kton/day (calculated) for ^{16}N in Super-Kamiokande [15], both before cuts normally designed to suppress these and other spallation products. Both ^{12}B ($T_{1/2} = 20.2\text{ms}$, $Q = 13.4\text{ MeV}$) and ^{16}N ($T_{1/2} = 7.13\text{s}$, $Q = 10.4\text{ MeV}$) are unstable to β^- decay, and their high production rates and endpoint energies make them significant backgrounds; the very long lifetime of ^{16}N makes it especially pernicious.

Section II describes our calculation of the production rate of the secondaries in muon showers. Section III offers a precise *ab initio* calculation of the ^{12}B production rate at different depths, and a direct comparison of our results with the measured production rate at the Kamioka depth measured by KamLAND. Section IV offers a similar calculation for the production rate of ^{16}N in water. We draw our conclusions in section V.

II. MUON PRODUCTION OF SECONDARIES

Using the known muon flux underground, we used FLUKA [16] to calculate the production rates, energies, and path lengths of all prominent secondaries, i.e.,

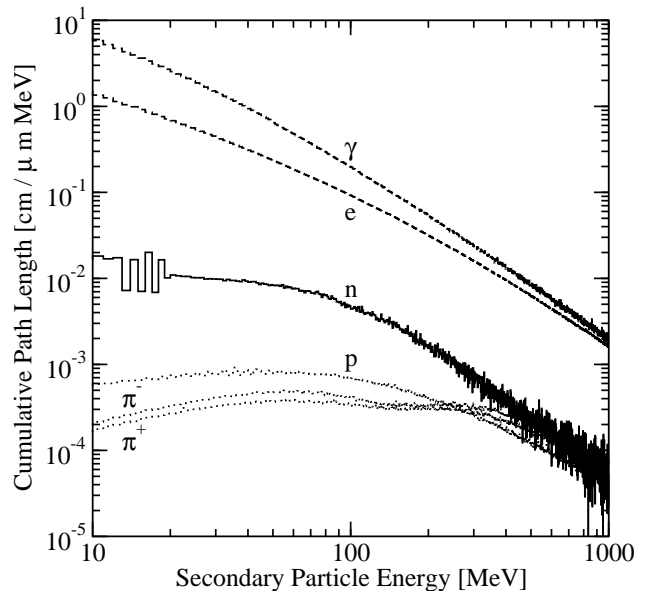


FIG. 1: Cumulative path length $dL(E)/dE$ of secondaries (in cm of path length per meter of μ track, and in secondary particle energy bins of 1 MeV) generated by muons at 285 GeV, appropriate to the depth of Kamioka.

γ rays, electrons (and positrons), neutrons, protons, and π mesons. The FLUKA program is a Monte Carlo code able to simulate particle showers by propagating particles according to standard interactions. The FLUKA code has been validated for its use in muon-induced showers in a number of studies. Most notably, Wang *et al.* [14] used FLUKA to reproduce experimental results of the production rate of neutrons by muons in liquid scintillator at several depths, and Kudryavtsev *et al.* [7] performed extensive studies on the energy spectrum and range of neutrons produced underground in cosmic-ray induced showers.

Our FLUKA-based code was developed in the context of a study of the production rate of ^{11}C cosmogenic isotopes in oil-based detectors underground [12].

We simulated showers originating from muons at several relevant energies: 100 GeV (corresponding to the beam experiment of Ref. [2]), and also the average muon energy at a depth of 500 m.w.e.), 285 GeV (the average energy at Kamioka), 320 GeV (the average energy at Gran Sasso), and 350 GeV (the average energy at Sudbury). The use of the average muon energy should be adequate given that the cross sections for muon-induced processes scale nearly like the energy [1]. Only μ^- were simulated, though the results (except for muon capture) would be very similar for μ^+ . The target material in the simulation was the solvent of the liquid scintillator for Borexino, trimethylbenzene (C_9H_{12}), with density 0.88 g/cm^3 (incidentally, this makes up 20% of the solvent used in KamLAND [9]). The results should not vary greatly with other organic solvents, given that typical values of the density and mass ratio between carbon

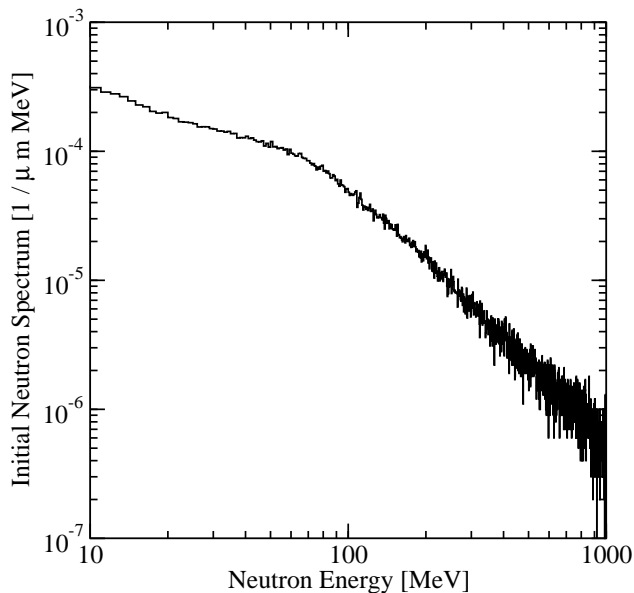


FIG. 2: Energy spectrum of neutrons (per meter of μ track, and in neutron energy bins of 1 MeV) produced by muons at 285 GeV, corresponding to Fig. 1.

and hydrogen are close to those of trimethylbenzene. Additionally, due to the similar relevant properties, the results for water should also be similar. We tracked muons for 100 meters, and for each of the prominent secondaries calculated the cumulative path of the particles as a function of the particle energy, with a 10 GeV upper cutoff.

As a representative example, in Fig. 1 we show results for secondaries below 1 GeV produced by muons at 320 GeV. For each particle, this figure shows the cumulative path length $dL(E)/dE$ traveled by all particles of that type at each 1 MeV bin of energy. The relative heights reflect both the particle multiplicities and also how much path length they accumulate at each energy (and hence on the mechanisms of energy and particle loss). The calculation includes all real secondary particles in the shower, including the abundant flux of bremsstrahlung photons from the muons. It is worthwhile to note that the usually-defined “range” of the secondary particles is not directly related to the cumulative path length as reported in Fig. 1: in fact, the trajectory of each secondary particle is broken in a large number of track segments, each one of them corresponding to the energy of the particle in that track segment; thus each secondary particle contributes to a large number of bins in the plot, from the initial energy down to lower energies as the particle gets slowed down along its track.

As noted, the neutron secondaries are of special practical importance, and here we focus just on them and the isotopes they produce by (n, p) reactions. Future studies which consider other produced isotopes will need to consider other secondaries too. In Fig. 2, we show the energy spectrum of the neutron secondaries. In this range, the neutron spectrum calculated here can be described as a

power law $\sim E^{-0.5}$ over ~ 10 – 100 MeV, and a power law $\sim E^{-2}$ over ~ 100 – 1000 MeV. Our results are consistent with those of Ref. [7], which are also based on a FLUKA calculation.

III. ^{12}B PRODUCTION IN OIL

A. Production Reaction (μ^- , ν_μ)

While at sea level, the capture of stopped μ^- on ^{12}C is the dominant means of producing ^{12}B , this is no longer true more than a few hundred meters underground, due to the steeply falling fraction of stopping muons.

The rate of stopping muons as a function of depths was inferred from the muon flux reported in Table I and from the ratio of stopping to throughgoing muons from Ref. [17]. At the Kamioka depth the expected rate of stopping muons is about 365/kton/day (this is consistent with the Super-Kamiokande measurement of 220/kton/day, after taking into account the detection efficiency of 0.65 [18]). Only negative muons can undergo nuclear capture, and the fraction of negative muons is 44% [18]. The fraction of negative muons undergoing capture on ^{12}C in hydrocarbons is 7.7% [19, 20]. For muons undergoing capture, the branching ratio in the channels resulting in production of a bound ^{12}B state is 18.6% [20]. Thus the expected production rate of ^{12}B in KamLAND amounts to 2.3/kton day.

The expected rate of ^{12}B production by μ^- capture at other depths was also calculated similarly, and the results are summarized in Table II. It is important to bear in mind that beyond about 500 m.w.e., the muon average energy and hence all secondary production rates quoted per meter of muon track, vary only slowly with depth. Accordingly, the focus of this paper is the relative rates of different secondary interactions.

At shallow depths, where the $^{12}\text{C}(\mu^-, \nu_\mu)$ channel is important, its rate can be very large. For example, the ^{12}B rate is about 11 Hz in the inner 0.680 kton of Mini-BooNE (at sea level), where it is a significant background for the supernova detection trigger [21].

B. Production Reaction (n, p)

To evaluate the contribution from (n, p) reactions, we used a technique originally developed to calculate the production rate of the ^{11}C isotope in organic liquid scintillators [22], and recently exploited to calculate the production rate of cosmogenic isotopes in xenon detectors [23]. As shown in Fig. 1, one of the key results obtained with the FLUKA calculation is the cumulative path length traveled by secondaries of each type and energy. Using this, the effects of reactions of the secondaries can be calculated easily, without modifying their transport in FLUKA, provided that the reactions considered are much

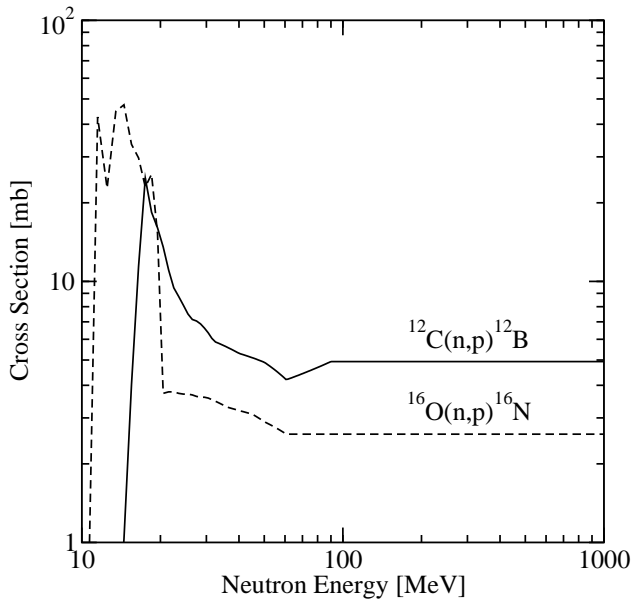


FIG. 3: Cross sections for $^{12}\text{C}(n,p)^{12}\text{B}$ and $^{16}\text{O}(n,p)^{16}\text{N}$ as a function of the neutron energy in the lab frame. Data were available up to about 90 MeV for ^{12}C and 60 MeV for ^{16}O , beyond which we assumed the cross sections remain constant.

less important than the dominant particle stopping reactions. For example, for ~ 10 – 100 MeV neutrons, the (n,p) cross sections considered here are ~ 10 mb, much smaller than the total nuclear cross sections of ~ 1 b.

For a secondary particle of energy E , denote the isotope production cross section by $\sigma(E)$, and the appropriate target density by n , so that the mean free path is $\lambda(E) = [n\sigma(E)]^{-1}$. Thus given the cumulative path length $dL(E)/dE$ calculated with FLUKA, the expected number of interactions of this type at an energy E (and per energy range dE) is simply $[dL(E)/dE]/\lambda(E)$. It is important to emphasize that the quantity $dL(E)/dE$ is *not* the distance traveled by a secondary of initial energy E ; in that case, the dominant stopping reactions would slow the secondary and reduce its interaction rate. Instead, $dL(E)/dE$ is the total amount of path length accumulated by all secondaries of this type, while they were at the energy E .

We will indicate with R_T the total expected number of interactions, and hence the isotope production rate, given in units of per muon track length. The probability for each secondary to have an interaction in one of the channels of interest and to produce the cosmogenic isotopes under study here is much smaller than unity, given that the cross sections for the processes of interest are negligible with respect to the cross sections of the dominant particle stopping reactions. Therefore we can make the following approximation:

$$R_T \simeq \int dE \frac{dL(E)}{dE} [n\sigma(E)]. \quad (1)$$

Note that the initial secondary particle energy spectrum

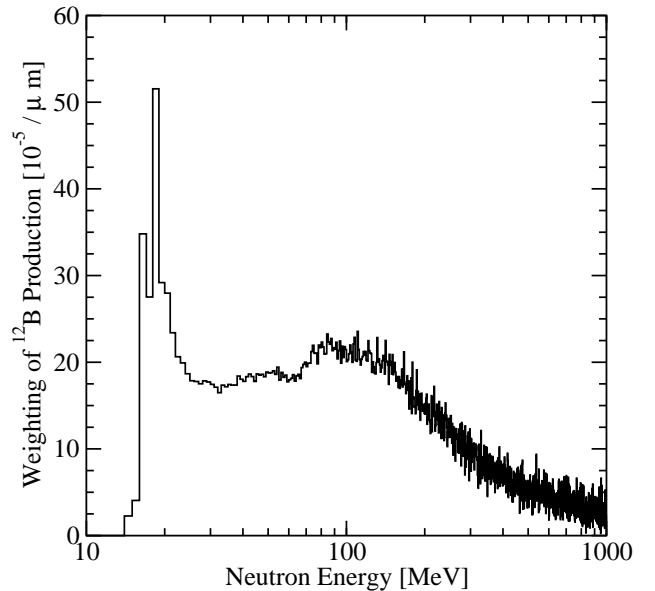


FIG. 4: Relative weighting of the $^{12}\text{C}(n,p)^{12}\text{B}$ production, considered as an integral in $d \log E$ (though the data points are evaluated in linear steps of 1 MeV), for neutrons generated in showers induced by muons at 285 GeV.

is not used here directly, but only as an input to the second step of the FLUKA calculation, which handles all of the particle stopping reactions after having generated the secondaries. The relative weighting of the integral is most conveniently displayed with the energy on a logarithmic scale, i.e., in terms of $d \log E \sim dE/E$, the shape of this integrand:

$$R_T \sim \int d \log E \left[E \frac{dL(E)}{dE} \sigma(E) \right]. \quad (2)$$

In this paper, we consider just the (n,p) reactions for secondary neutrons. However, for any secondary particle, any reaction which can be considered as a perturbation to the main particle stopping reactions could be treated very similarly.

Returning to the particular case of $^{12}\text{C}(n,p)^{12}\text{B}$, the cross section was compiled from a number of references [24] and is shown in Fig. 3. The same figure also includes the cross section for the process $^{16}\text{O}(n,p)^{16}\text{N}$, also compiled from a number of references [25].

As noted, a full simulation of muon-induced showers was performed with FLUKA [16], leading to Fig. 1. The product of these two figures and the energy E (i.e., considered as an integral in $d \log E$) is shown in Fig. 4, showing that for this reaction, the most important neutron energies are ~ 10 – 100 MeV, probing a crucial region of the neutron spectrum shown in Fig. 2. For each decade or fraction thereof in neutron energy, the relative contribution to the integral can be immediately estimated by the relative height of the displayed curve. Due to the (n,p) cross section threshold, this reaction is insensitive to the very numerous soft neutrons.

TABLE II: Production rates for ^{12}B in muon induced showers at different depths D , given both per muon track length, and per volume and time. The experimental number reported by KamLAND [13] is also noted for comparison.

D [m.w.e.]	0	500	2700	3800	6000
$\langle E_\mu \rangle$ [GeV]	4	100	285	320	350
Process	Rate [$10^{-5}/\mu\text{m}$]				
(n,p)	1.0	10.2	26.9	31.2	32.2
(μ^-, ν_μ)	12.6	2.3	0.9	0.8	0.8
Process	Rate [events/kton day]				
(n,p)	1.4×10^9	1480	61.3	8.9	0.1
(μ^-, ν_μ)	2.1×10^6	390	2.3	0.3	0.003
Total	2.2×10^6	1870	63.6	9.2	0.1
Measured	60				

C. Other Production Reactions

We also examined the production channels triggered by π^- interactions: ^{12}B can be produced either by π^- capture or by π^+ photoproduction, $^{12}\text{C}(\gamma, \pi^+)^{12}\text{B}$. The number of π^- produced in muon-induced showers at the Kamioka depth is $4.4 \times 10^{-3}/\mu\text{m}$. The fraction of stopping pions producing ^{12}B isotopes in carbon is 9.7×10^{-4} [26]. The rate of ^{12}B production through π^- capture is less than $4 \times 10^{-6}/\mu\text{m}$ and therefore negligible with respect to the two main channels. Concerning the $^{12}\text{C}(\gamma, \pi^+)^{12}\text{B}$ exchange reaction, the cross section is $\sim 1\mu\text{b}$ above a threshold of 155 MeV [27], and thus the yield through this channel is negligible.

Production of ^{12}B in organic liquid scintillators can also happen by interaction on the target ^{13}C . The low natural isotopic abundance of ^{13}C (1.1% [28]) and the rate of the cosmogenic reaction $^{12}\text{C} \rightarrow ^{11}\text{C}$ [22], also resulting in the net loss of a nucleon from the original isotope, suggest that the production rates through these channels are negligible.

D. Total Rates for ^{12}B Production

In Table II, we summarize the ^{12}B production rates at different depths. For the four underground depths, the (n,p) results were obtained by direct calculations with FLUKA, as described. At sea level, the result was estimated by scaling the neutron production cross section as $\sigma \propto E^\alpha$ [1]. The value chosen for the α is the average of the measured values on a number of unstable isotopes produced on ^{12}C in the beam experiment at CERN: $\alpha = 0.73$ [2]. The depth dependence of the (μ^-, ν_μ) results was obtained using the stopping muon fractions given by Ref. [17]. Also in Table II, the rates per volume R_V were obtained by

$$R_V = R_T \Phi_\mu (M_D/\rho) \beta, \quad (3)$$

where R_T is the rate per muon track length, Φ_μ is the muon flux, M_D the detector mass, ρ the mass density,

TABLE III: Production rates for ^{16}N in muon induced showers at different depths D , given both per muon track length, and per volume and time.

D [m.w.e.]	0	500	2700	3800	6000
$\langle E_\mu \rangle$ [GeV]	4	100	285	320	350
Process	Rate [$10^{-5}/\mu\text{m}$]				
(n,p)	0.8	9.1	23.0	25.6	26.3
(μ^-, ν_μ)	19.7	3.6	1.4	1.3	1.3
Process	Rate [events/kton day]				
(n,p)	1.1×10^9	1320	52.4	7.3	0.07
(μ^-, ν_μ)	2.8×10^6	530	3.2	0.4	0.004
Total	2.9×10^6	1850	55.5	7.7	0.08

and β a correction factor to compensate for averaging over the muon spectrum [2]:

$$\beta = \frac{\langle E_\mu^\alpha \rangle}{\langle E_\mu \rangle^\alpha} = 0.87 \pm 0.03. \quad (4)$$

Because of how we have defined our inputs, the factor β is only needed for the (n,p) calculations.

From the values listed in Table II, one can see that the dominant process for the production of ^{12}B at depths greater than a few hundred meters is the (n,p) exchange reaction, the (μ^-, ν_μ) reaction becoming much less important. The systematic error on the production rate quoted in Table II due to the uncertainty on the (n,p) cross sections is estimated to be about 5%. Other uncertainties and approximations probably increase this, but nevertheless, the calculation is in excellent agreement with the rate measured at 2700 m.w.e. depth in KamLAND [13]. This agreement is an important confirmation of entire procedure for calculating both the secondaries produced by muons, as well as the interactions of those secondaries.

The sea-level calculations should be taken only as crude estimates, since one would have to properly take into account the shielding of the detectors, non-vertical muons, unattenuated hadronic cosmic rays, etc. Additionally, most detectors on the surface are very small, so that the showers induced by muons would not be fully contained; conversely, the small size means little shielding from interactions outside the detector. As an example of the importance of the ^{12}B production rates and mechanisms, we note that the proposal of Ref. [29] to measure reactor $\bar{\nu}_e + e^- \rightarrow \bar{\nu}_e + e^-$ scattering as a test of $\sin^2 \theta_W$; the signal is a single scattered electron, and there is a background from ^{12}B beta decays [29].

IV. ^{16}N PRODUCTION IN WATER

Following the same procedure as above, we also calculated the production rates of ^{16}N in a water-based detector. The two production channels taken into consideration are $^{16}\text{O}(n,p)^{16}\text{N}$ and $^{16}\text{O}(\mu^-, \nu_\mu)^{16}\text{N}$. The cross section data for $^{16}\text{O}(n,p)^{16}\text{N}$ are shown in Fig. 3. Note

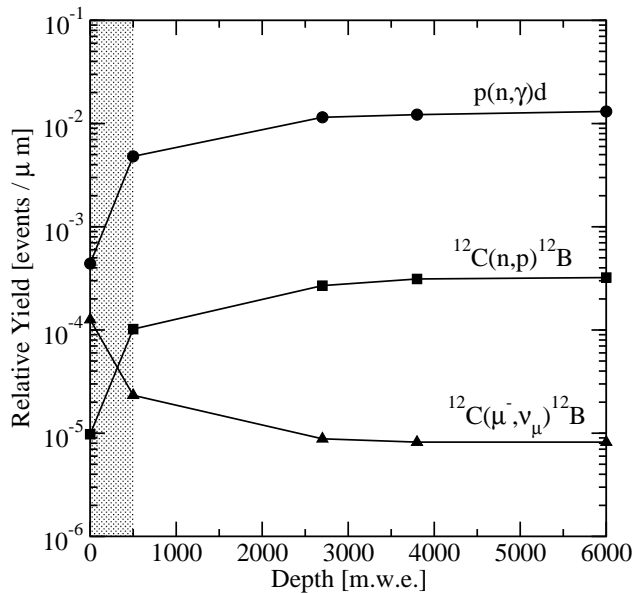


FIG. 5: Yields for neutron capture, $^{12}C(n,p)^{12}B$, and $^{12}C(\mu^-, \nu_\mu)^{12}B$, as a function of depth, in units of per muon track length. In the shaded region below 500 m.w.e., the values and their variation with depth should be taken only as crude estimates.

that by comparing the cross sections on ^{12}C and ^{16}O , a somewhat lower range of neutron energies is relevant in the latter case. The fraction of stopping negative muons undergoing capture on ^{16}O in water 18.4% [19], and the fraction of these ending in the ground state of ^{16}N is 10.7% [20]. Results for the production rates of ^{16}N are given in Table III.

V. CONCLUDING REMARKS

In this paper we present a study of the production mechanism of the ^{12}B isotope in oil-based (organic liquid scintillator) detectors, and also of the ^{16}N isotope in water-based detectors. At depths more than a few hundred m.w.e. underground, their production is almost completely via (n,p) reactions initiated by fast muon-induced neutrons. We performed an *ab initio* calculation of the production rates and compared the calculated total production rate for ^{12}B with data measured in KamLAND, obtaining excellent agreement. The paper offers a further validation of the technique exploited for the calculation of the rate of production of cosmogenic isotopes, which was previously developed in the context of the study of the ^{11}C rate in oil detectors [12] and of several cosmogenic isotopes in xenon [23].

In Fig. 5 we show the variation with depth of three reaction rates in oil-based detectors:

1. The $^{12}C(\mu^-, \nu_\mu)^{12}B$ rate, a measure of the muon flux, which is well measured and understood [17].

2. The $p(n,\gamma)d$ rate, a measure of the muon-induced soft-neutron flux, which is reasonably well measured and understood [30].
3. The $^{12}C(n,p)^{12}B$ rate, a measure of the muon-induced moderate-energy neutron flux, which is uncertain [14]; it is quite significant that the point at 2700 m.w.e. has been confirmed by KamLAND [13].

The curves for water-based detectors are similar.

Based on these results, we note that the depth dependence of these reactions is both mild and well-understood. Accordingly, we place the most significance on the *relative heights* of the curves in Fig. 5. Thus in terms of further testing of the muon-induced backgrounds underground, it is difficult to make progress by trying to measure the mild depth dependence more precisely. Instead, it would likely be much more fruitful to measure isotope production ratios at a fixed (or extrapolated) depth, since these vary by orders of magnitude, not factors of 2. These orders of magnitude reflect both the strong variation of the secondary spectra with energy, as well as the energy dependence of the associated isotope production reactions. For example, a measurement of the ^{12}B production rate, especially relative to the total neutron capture rate, directly probes the 10–100 MeV neutron flux.

Thus, it would be very valuable if the KamLAND, Super-Kamiokande, and the Sudbury Neutrino Observatory experiments were to publish their detailed results on the relative yields of unstable isotopes produced by muons, as a function of distance from the muon track. It would be especially useful to have results on the correlations in particle yields, i.e., which isotopes (including neutrons) accompany each other in a given spallation interaction, and at what distances. In the Sudbury Neutrino Observatory, absolute muon rates are very low, which restricts the possible statistics; however, since their intrinsic and muon background rates are so low, there is a unique opportunity to measure all detector activity following a muon out to very large distances and times.

The development of a well-tested physical model for all secondaries induced by muons would very likely allow more precise cuts in existing experiments, some of which have $\sim 20\%$ deadtime due to cuts following muons. It would also lead to better design considerations for future experiments pursuing greater sensitivity for reactor neutrinos [31], low-energy solar neutrinos [32], the diffuse supernova neutrino background [34], double beta decay [33], and dark matter [35].

Acknowledgments

We thank A. Ianni, V. Kudryavtsev, J. Orrell, A. Pocar, and P. Vogel for reading the manuscript and for useful comments. The work of C.G. was supported in part by the U.S. National Science Foundation under grant PHY-0201141. The work of J.F.B. was supported by The Ohio State University.

- [1] O.G. Ryazhskaya and G.T. Zatsepin, *Izv. Akad. Nauk USSR Ser. Fiz.* **29**, 1946 (1965).
- [2] T. Hagner *et al.*, *Astropart. Phys.* **14**, 33 (2000).
- [3] MACRO Collaboration, M. Ambrosio *et al.*, *Astropart. Phys.* **10**, 11 (1999).
- [4] M. Cribier *et al.*, *Astropart. Phys.* **6**, 129 (1997).
- [5] C. Waltham *et al.*, *Through-Going Muons in the Sudbury Neutrino Observatory*, Proceedings of the International Cosmic Ray Conference, Hamburg 2001, Copernicus Gesellschaft editor (2001).
- [6] N. Tagg, *The ^8Li calibration source and through-going muon analysis in the Sudbury Neutrino Observatory*, Ph.D Dissertation, University of Guelph (2001).
- [7] V.A. Kudryavtsev, N.J.C. Spooner, and J.E. McMillan *Nucl. Inst. Meth. A* **505**, 688 (2003).
- [8] S. Eidelman *et al.*, *Phys. Lett. B* **592**, 1 (2004).
- [9] KamLAND Collaboration, K. Eguchi *et al.*, *Phys. Rev. Lett.* **90**, 021802 (2003); KamLAND Collaboration, K. Eguchi *et al.*, *Phys. Rev. Lett.* **92**, 071301 (2004).
- [10] Borexino Collaboration, G. Alimonti *et al.*, *Astropart. Phys.* **16**, 205 (2002).
- [11] M. Deutsch, *Proposal to NSF for a Borexino Muon Veto*, Massachusetts Institute of Technology (1996).
- [12] C. Galbiati, *Data taking and analysis of the Counting Test Facility of Borexino*, Tesi di Dottorato, Università degli Studi di Milano (1999).
- [13] KamLAND Collaboration, T. Araki *et al.*, *Phys. Rev. Lett.* **94**, 081801 (2005).
- [14] Y-F. Wang *et al.*, *Phys. Rev. D* **64** 013012 (2001).
- [15] Super-Kamiokande Collaboration, Y. Gando *et al.*, *Phys. Rev. Lett.* **90**, 171302 (2003); Y. Koshio, *Study of solar neutrinos at Super-Kamiokande*, PhD Thesis, University of Tokyo (1998).
- [16] A. Fassò *et al.*, *Electron-photon transport in FLUKA: Status*, Proceedings of the MonteCarlo 2000 Conference, Lisbon, October 23-26 2000, A. Kling, F. Barao, M. Nakagawa, L. Tavora and P. Vaz eds., Springer-Verlag Berlin, p. 159 (2001); Fassò A *et al.*, *FLUKA: Status and Prospective for Hadronic Applications*, Proceedings of the MonteCarlo 2000 Conference, Lisbon, October 23-26 2000, A. Kling, F. Barao, M. Nakagawa, L. Tavora and P. Vaz eds., Springer-Verlag Berlin, p. 955 (2001).
- [17] G.L. Cassiday, J.W. Keuffel, and J.A. Thompson, *Phys. Rev. D* **7**, 2022 (1973).
- [18] Super-Kamiokande Collaboration, E. Blaufuss *et al.*, *Nucl. Inst. Meth. A* **458**, 638 (2001).
- [19] T. Suzuki, D.F. Measday, and J.P. Roalsvig, *Phys. Rev. C* **35**, 2212 (1987).
- [20] D.F. Measday, *Phys. Rep.* **354**, 243 (2001).
- [21] M.K. Sharp, J.F. Beacom, and J.A. Formaggio, *Phys. Rev. D* **66**, 013012 (2002).
- [22] C. Galbiati *et al.*, *Phys. Rev. C* **71**, 055805 (2005).
- [23] T. Bender, *Cosmogenic nuclide production in liquid xenon*, Fall Semester Junior Project, Princeton University (2005).
- [24] D.A. Kellogg, *Phys. Rev.* **90**, 224 (1953); W.E. Kreger and B.D. Kern, *Phys. Rev.* **113**, 890 (1959); E.M. Rimmer and P.S. Fisher, *Nucl. Phys. A* **108**, 567 (1968); V.V. Bobyr *et al.*, *Izv. Ros. Akad. Nauk, Ser.Fiz.*, **36**, 2621 (1972); M.W. McNaughton, N.S.P. King, F.P. Brady, and J.L. Ullmann, *Nucl. Inst. Meth.* **129**, 241 (1975); P.J. Dimbylow, *Phys. Med. Biol.* **25**, 637 (1980); A. Debroux *et al.*, *Phys. Rev. C* **25**, 2883 (1982); K.P. Jackson *et al.*, *Phys. Lett. B* **201**, 25 (1988); J. Mildemberger *et al.*, *Phys. Rev. C* **42**, 732 (1990); F.P. Brady *et al.*, *Phys. Rev. C* **43**, 2284 (1991).
- [25] B.L. Cohen, *Phys. Rev.* **81**, 184 (1951); E.B. Paul and R.L. Clarke, *Can. Jour. Phys.* **31**, 267 (1953); H.C. Martin, *Phys. Rev.* **93**, 498 (1954); J. Kantele and D.G. Gardner, *Nucl. Phys.* **35**, 353 (1962); J.A. DeJuren and R.W. Stooksberry, *Phys. Rev.* **120**, 901 (1960); J.A. DeJuren, R.W. Stooksberry and M. Wallis, *Phys. Rev.* **127**, 1229 (1962); G. Paic, I. Slaus, and P. Tomas, *Phys. Lett.* **9**, 147 (1964); R. Prasad and D.C. Sarkar, *Nucl. Phys.* **85**, 476 (1966); B. Mitra and A.M. Ghose, *Nucl. Phys.* **83**, 157 (1966); M. Schmidt-Hoenow and W. Herr, *Radiochimica Acta* **17**, 142 (1972); P.J. Dimbylow, *Phys. Med. Biol.* **25**, 637 (1980); G.A. Needham *et al.*, *Nucl. Phys. A* **385**, 349 (1982); K.H. Hicks *et al.*, *Phys. Rev. C* **43**, 2554 (1991); M. Subashi *et al.*, *Nucl. Sci. Eng.* **135**, 260 (2000).
- [26] J.S. Bistirlich, K.M. Crowe, A.S.L. Parsons, P. Skarek, and P. Truoeel, *Phys. Rev. Lett.* **25**, 689 (1970); W. Maguire and C. Werntz, *Nucl. Phys.* **A205**, 211 (1973).
- [27] F.L. Milder *et al.*, *Phys. Rev. C* **19**, 1416 (1979).
- [28] *Table of Isotopes*, 7th edition, edited by C.M. Lederer and V.S. Shirley, Wiley-Interscience Publisher, New York (1978).
- [29] J.M. Conrad, J.M. Link, and M.H. Shaevitz, *Precision measurement of $\sin^2 \theta_W$ at a reactor*, arXiv:hep-ex/0403048v3.
- [30] F. Boehm *et al.*, *Phys. Rev. D* **62**, 092005 (2000).
- [31] K. Anderson *et al.*, *White paper report on using nuclear reactors to search for a value of θ_{13}* , arXiv:hep-ex/0402041; E. A. K. Abouzaid *et al.*, "Report of the APS Neutrino Study Reactor Working Group," LBNL-56599.
- [32] H. Back *et al.*, "Report of the solar and atmospheric neutrino experiments working group of the APS multidivisional neutrino study," arXiv:hep-ex/0412016.
- [33] C. Aalseth *et al.*, arXiv:hep-ph/0412300.
- [34] J. F. Beacom and M. R. Vagins, *Phys. Rev. Lett.* **93**, 171101 (2004); S. W. Barwick *et al.*, "APS neutrino study: Report of the neutrino astrophysics and cosmology working group," arXiv:astro-ph/0412544.
- [35] See, e.g., H. Wulandari, J. Jochum, W. Rau and F. von Feilitzsch, "Neutron background studies for the CRESST dark matter experiment," arXiv:hep-ex/0401032; J. M. Carmona *et al.*, *Astropart. Phys.* **21**, 523 (2004); M. J. Carson *et al.*, *Astropart. Phys.* **21**, 667 (2004); P. F. Smith, D. Snowden-Ifft, N. J. T. Smith, R. Luscher and J. D. Lewin, *Astropart. Phys.* **22**, 409 (2005); C. Bungau *et al.*, *Astropart. Phys.* **23**, 97 (2005); M. J. Carson *et al.*, "Simulations of neutron background in a time projection chamber relevant to dark matter searches," arXiv:hep-ex/0503017.